

Article

Effect of Multi-Pass Caliber Rolling on Dilute Extruded Mg-Bi-Ca Alloy

Shuaiju Meng ^{1,2}, Hui Yu ^{1,*}, Haisheng Han ^{1,3,*}, Jianhang Feng ³, Lixin Huang ⁴, Lishan Dong ^{1,*}, Xiaolong Nan ⁵, Zhongjie Li ⁶, Sung Hyuk Park ⁷ and Weimin Zhao ^{1,*}

¹ School of Materials Science and Engineering, Hebei University of Technology, Tianjin 300130, China; shuaijumeng@163.com

² Magnesium Department, Korea Institute of Materials Science, Changwon 51508, Korea

³ Tianjin Key Laboratory of Materials Laminating Fabrication and Interfacial Controlling Technology, Tianjin 300130, China; 13933765819@126.com

⁴ CITIC Dicastal Co., LTD, Qin Huangdao 066011, Hebei, China; huanglixin@dicastal.com

⁵ National Key Laboratory of Shock Wave and Detonation Physics, Institute of Fluid Physics, China Academy of Engineering Physics, Mianyang 621999, China; Nanxl@caep.cn

⁶ School of Materials Science and Engineering, Shanngshai Jiao Tong University, Shuanghai 200240, China; lizhongjie1993@126.com

⁷ School of Materials Science and Engineering, Kyungpook National University, Daegu 41566, Korea; sh.park@knu.ac.kr

* Correspondence: yuhuidavid@126.com (H.Y.); hanhaisheng@hebut.edu.cn (H.H.); donglishan1991@163.com (L.D.); wmzhao@hebut.edu.cn (W.Z.)

Received: 12 January 2020; Accepted: 26 February 2020; Published: 2 March 2020



Abstract: A Mg-1.32Bi-0.72Ca (BX11) alloy having bimodal grain structure was successfully prepared by a novel processing route of combining extrusion and three-pass caliber rolling. The first extruded and then caliber-rolled (E-CRed) alloy demonstrates a necklace-like grain structure with ultrafine grains formed around the microscale deformed grains, which is remarkably different from the uniform microstructure of the as-extruded alloy. In addition, the E-CRed BX11 alloy exhibits strong basal texture which is mainly original from the microscale deformed grains. Furthermore, the E-CRed BX11 alloy demonstrates excellent comprehensive mechanical properties, with an ultra-high yield strength of 351 MPa and a good elongation to failure of 13.2%. The significant strength improvement can be mainly attributed to the significant grain refinement and much stronger basal texture compared with the as-extruded sample.

Keywords: Mg-Bi-Ca; mechanical property; bimodal microstructure

1. Introduction

Magnesium (Mg) alloys with advantages of low density have great potentials to be used in transport vehicles for weight-saving. Improving the mechanical properties of the Mg alloys is considered as an essential issue for their wider usage at present because of their relatively poor mechanical performance compared with steel, titanium alloys, and aluminum alloys [1–3]. There have been numerous studies focused on the development of new Mg alloys with good mechanical properties via various methods, including alloying strategies and advanced processing technology. Until now, high strength has been achieved in Mg-Al [4,5], Mg-Zn [6–8], Mg-Ca [9,10], and Mg-Sn [11,12]-based alloys by incorporating grain refinement, precipitation hardening, and texture hardening. The Mg-Bi alloy system also shows typical precipitation-type phase equilibrium and several Mg-Bi-based alloys with attractive mechanical properties have been fabricated in recent years [13–16]. For example, the Mg-5Bi-1Ca/Si (all compositions quoted in this work are in wt. % unless otherwise stated) alloy exhibiting a tensile

elongation (EL) of over 40% has been fabricated by Remennik et al. [13] through the rapid solidification (RS) and extrusion process. In addition, Somekawa et al. [14] found that low temperatures (105–210 °C) extruded Mg-2.5Bi alloy, demonstrated a room temperature tensile EL of 170%. On the other hand, the processing route of low temperature extrusion [14] or RS-involved extrusion [13] is not commercially acceptable for the mass production of Mg alloys to date. In this respect, a dilute Mg-Bi-Ca alloy was successfully fabricated by single-step conventional extrusion processing [17]. However, the strength of the as-extruded Mg-Bi-Ca alloy is too low, with the yield strength (YS) of only 135 MPa, and further enhancement on the strength of the BX11 alloy is urgently expected.

Recently, caliber rolling has been introduced as one of the modified rolling processes that can be used for the mass production of Mg-based materials containing ultra-fine grains with high strength. Until now, there have been several researches focused on enhancing the mechanical properties of Mg alloys by caliber-rolling processing [18–21]. Somekawa et al. [18] found that the YS of as-extruded Mg-Zn, Mg-Al, Mg-Ca, Mg-Sn, and Mg-Y binary alloys could be significantly improved after 4 or 14-pass caliber-rolling processing. Lee et al. [19] reported that seven-pass CRed AZ31 alloy demonstrated YS, ultimate tensile strength (UTS), and EL of 298 MPa, 378 MPa, and 20.9%, respectively. Later, they further [20] fabricated an ZK60 alloy with ultra-fine grain microstructure, yielding a YS of 364 MPa, UTS of 389 MPa, and an EL of 18% by six-pass caliber rolling. Mukai et al. [21] reported the weakening of the basal texture and enhancement of YS when applying the caliber rolling to the AZ31 alloy. All these works demonstrated the great potential of caliber rolling in enhancing the mechanical properties of the Mg alloy, but the pass number of caliber rolling is too many, which inevitably leads to the decrease of production efficiency and increase of cost.

Therefore, in this study, we attempted to improve the strength of as-extruded Mg-Bi-Ca alloy by simple three-pass caliber rolling. Besides, the relevant strengthen mechanism will also be discussed based on the microstructure characterization.

2. Materials and Methods

The extruded rod with the dimension of Φ 10 mm \times L 60 mm and chemical composition of Mg-1.32Bi-0.72Ca wt. % (hereafter denoted as BX11) was used as the rolling blank. The processing method and parameters of fabricating the as-extruded BX11 rod was described in our former research [17]. As illustrated in Figure 1, the caliber-rolling process was carried out at temperature of 300 °C with grooves size from 9.6 mm to 7.9 mm, and the area reduction of the 3-pass caliber rolling is ~25%, corresponding to a strain $\epsilon_{CR} = -\ln(A/A_0)$, where A_0 and A are the cross-sectional area of the initial extruded billet and the caliber-rolled rod, respectively, of 22.3%. The rod was rotated between the passes of the caliber-rolling progress, and after the third pass rolling, the sample was air-cooled to room temperature. For the tensile property test, the dog bone-shaped tensile specimens with gage diameters of 4 mm and lengths of 16 mm were machined. Room temperature tensile tests for E-CRed samples along the rolling direction (RD) were carried out at a strain rate of $1 \times 10^{-3} \text{ s}^{-1}$ in the SUNS-UTM5105X testing machine (SHENZHEN SUNS TECHNOLOGY STOCK CO., LTD., Shenzhen, Guangdong, China), having 100 kN load capacity. The mechanical properties of as-extruded BX11 free from caliber rolling were also tested as a benchmark. All samples were tested at least three times to confirm the repeatability of the tensile properties.

In order to analyze the strength mechanism, microstructure characterization was carried out by Olympus BX51M light microscope (LM; OLYMPUS, Tokyo, Japan), JEOL JSM-7000F scanning electron microscope (SEM, JEOL Ltd., Tokyo, Japan) equipped with an energy dispersive spectrometer (EDS) and a Tecnai G² 20 transmission electron microscope (TEM, FEI Company, Hillsboro, OR, USA) equipped with energy-dispersive X-ray spectroscopy (EDX). Metallographic samples for microstructure characterization were cut from the as-extruded and the center part of the E-CRed BX11 alloy along the extrusion direction (ED) and RD, respectively. In order to figure out the phases in the specimen, X-ray diffraction (XRD) analysis was conducted using Bruker D8 Focus (Bruker AXS GmbH, Oestliche Rheinbrueckenstr, Karlsruhe, Germany). A solution made of 4.2 g picric acid, 70 mL ethanol, 10 mL

acetic acid, and 10 mL distilled water was adopted to etch the specimens for LM and SEM observation. For EBSD examination, the specimen surface was, firstly, mechanically ground, then polished by colloidal silica for 30 min. HKL Chanel 5 analysis software was used to analyze the EBSD data. In terms of TEM observations, the related thin disc samples with a diameter of 3 mm were mechanically polished to a thickness less than 200 μm , followed by ion milling using a GATAN 691 Precision ion polishing system (Technoorg Linda Co. Ltd., Ipari Park utca, Budapest, Hungary).

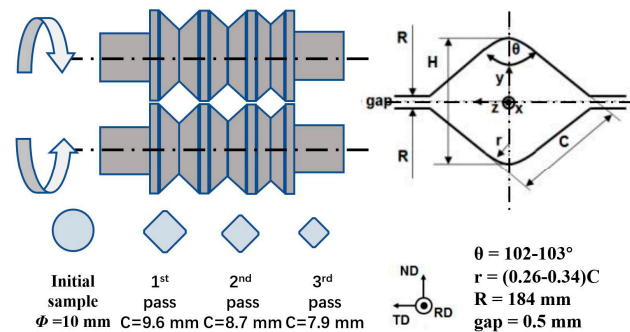


Figure 1. Schematic illustration of 3-pass caliber rolling. RD: rolling direction; ND: normal direction; TD: transverse direction.

3. Results and Discussion

3.1. Mechanical Properties

The tensile properties of the E-CRed BX11 alloy are given in Table 1, and the representative tensile stress-strain curves of the E-CRed BX11 alloy is presented in Figure 2a. An extraordinary combination of exceptionally high strength and good ductility is achieved in E-CRed BX11 alloy with the YS, UTS, and EL of 351 MPa, 381 MPa, and 13.2%, respectively. In addition, the stress-strain curves of the as-extruded BX11 free from caliber rolling is also included in Figure 2a for comparison. Before caliber rolling, BX11 alloy has a high ductility with EL of 43% but poor strength, with the YS of only 135 MPa. The YS of the E-CRed BX11 sample is more than two times higher than that of the as-extruded sample. Besides, the high YS of the E-CRed BX11 is much higher than that of the newly developed Mg-6Bi [16] and Mg-1Ca [22] binary alloys and is higher than that of more concentrated Mg-9.8Sn-1.2Zn-1Al [11] and Mg-8Bi-1Al-1Zn [15] samples. Furthermore, as demonstrated in Figure 2b [4,5,10,11,15,16,19,21–34], the YS of the E-CRed BX11 sample is even higher than those of some reported severe plastic deformation (SPD)-processed samples, including accumulative roll-bonding processed AZ91 [23], rolled and 7-pass CRed AZ31 [19], and 12-pass ECAPed Mg-3.7Al-1.8Ca-0.4Mn [24] alloys. On the other hand, although the ductility of the E-CRed BX11 is greatly decreased compared with the as-extruded sample, it is still much higher than those of most other ultra-high strength Mg alloys, as presented in Figure 2b. Compared with the newly fabricated Mg-3.5Al-3.3Ca-0.4Mn [5], Mg-2Sn-2Ca [25], and Mg-2Sn-1.95Ca-0.5Mn [26] alloys, which are reported having the three highest YSs in rare earth-free (RE-free) Mg alloys, the E-CRed BX11 alloy shows a little lower strength but much greater EL. Detailed microstructure characterization was conducted to explain the good mechanical performance of the E-CRed BX11 alloy, as presented in the following section.

Table 1. Tensile properties of E-CRed BX11 compared with the as-extruded sample.

Alloys	Process Parameters	YS ³ (MPa)	UTS ⁴ (MPa)	EL ⁵ (%)
BX11	E ¹ , 300 °C, 4 mm/s	135 ± 3	207 ± 4	43 ± 2
BX11	E-CRed ² , 300 °C	351 ± 3	381 ± 5	13.2 ± 2

¹ E: extrusion, ² CRed: caliber rolled, ³ YS: yield strength, ⁴ UTS: ultimate tensile strength, and ⁵ EL: elongation.

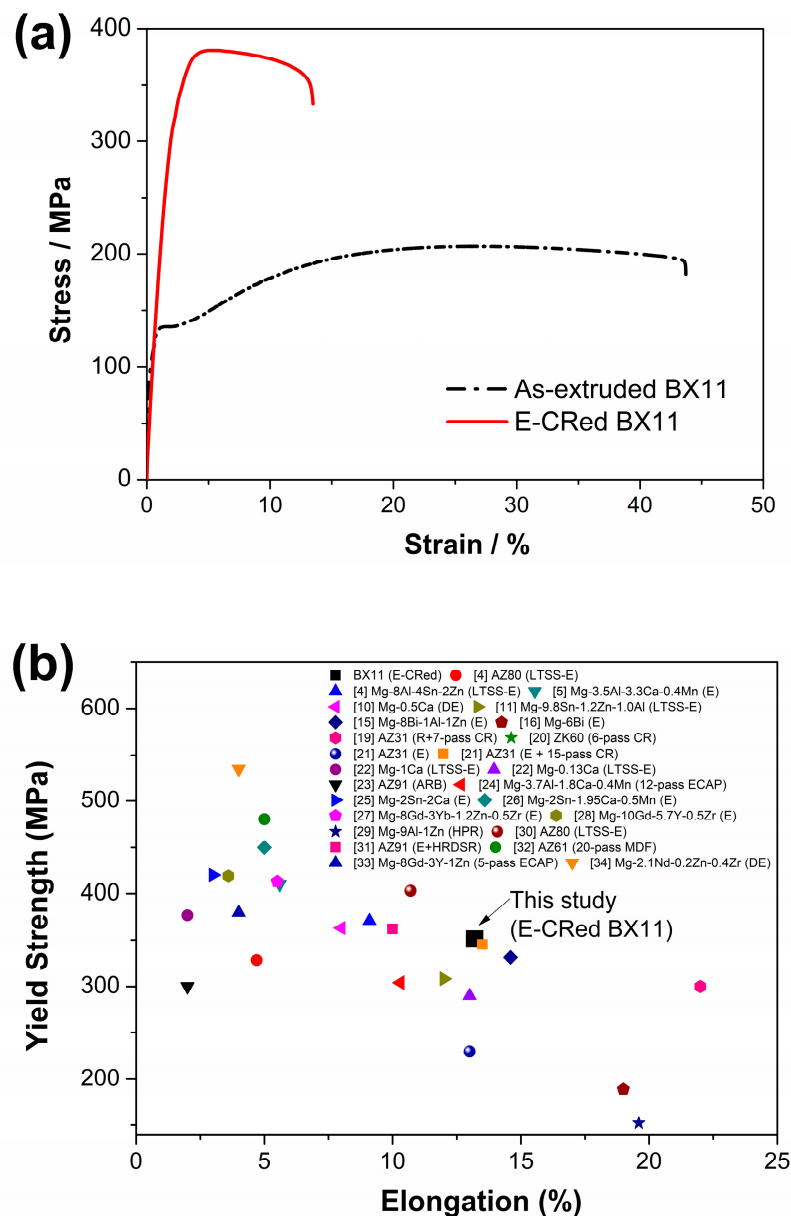


Figure 2. (a) Typical engineering tensile stress-strain curve of E-CRed BX11 alloy compared with the as-extruded sample, and (b) comparison of yield strength (YS) vs. elongation (EL) of various wrought Mg alloys [4,5,10,11,15,16,19,21–34]. (E: extrusion, CR: caliber rolling, LTSS-E: low temperature slow speed extrusion, DE: double extrusion, ARB: accumulative roll bonding, ECAP: equal channel angular pressing, HPR: hard plate rolling, HRDSR: high-ratio differential speed rolling, and MDF: multi-directional forging.)

3.2. Microstructure

As shown in Figure 3, the initial LM (Figure 3a and b) and SEM (Figure 3c) microstructure of the extruded rod consists of equiaxed grains, with average sizes of $\sim 6 \mu\text{m}$ along with some microscale second phases. The EDS analysis results of these second particles listed in Table 2 reveal that these second-phase particles consist of Mg-Bi and Mg-Bi-Ca compounds. Figure 4 shows the XRD results of the as-extruded sample; combined with the EDS results, the Mg-Bi and Mg-Bi-Ca particles dispersed in the matrix are determined as the Mg_3Bi_2 phase and $\text{Mg}_2\text{Bi}_2\text{Ca}$ phase, respectively. The result is consistent with that in previously fabricated Mg-5Bi-1Ca [13] and Mg-1.2Ca-12Bi alloys [35].

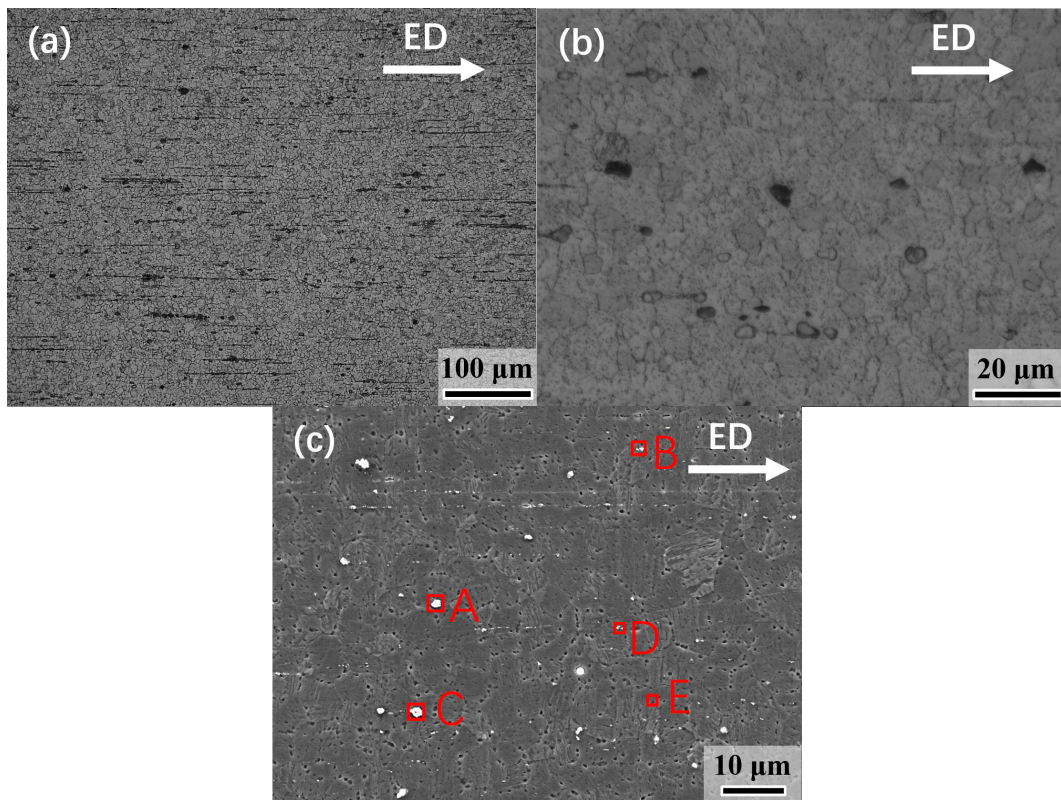


Figure 3. (a,b) Light microscope (LM) micrographs and (c) SEM images of as-extruded BX11 alloy.

Table 2. Energy dispersive spectrometer (EDS) results of the particles in the matrix of as-extruded BX11 alloy.

Area	Composition (wt. %)		
	Mg	Ca	Bi
A	76.34	6.33	17.33
B	73.48	0	26.52
C	93.60	2.27	4.13
D	93.90	0	6.10
E	99.73	0.27	0

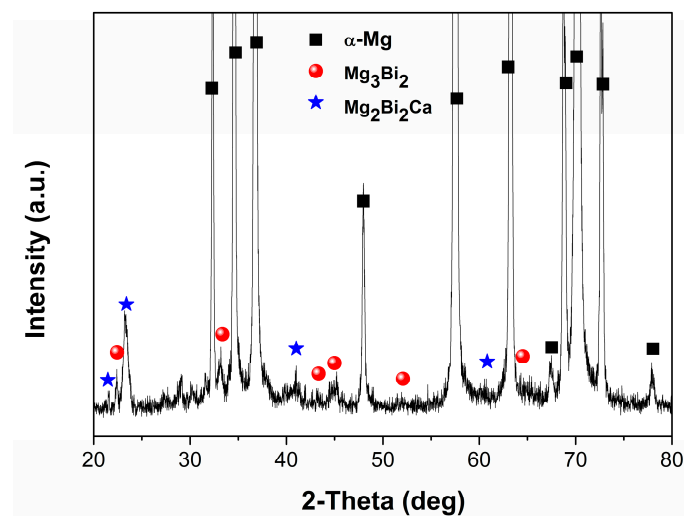


Figure 4. X-ray diffraction (XRD) pattern of as-extruded BX11 alloy.

Figure 5. shows the LM microstructure of the E-CRed sample. The E-CRed BX11 sample demonstrates a bimodal structure consisting of deformed grains and ultra-fine grains along the initial grain boundaries, suggesting that dynamic recrystallization (DRX) occurred during the three-pass caliber rolling at 300 °C. It should be noted that the bimodal grain structure is obviously different with that of the low temperature and slow speed extruded (LTSS-Eed) AZ80 [30], in which the deformed grains are greatly elongated and much larger.

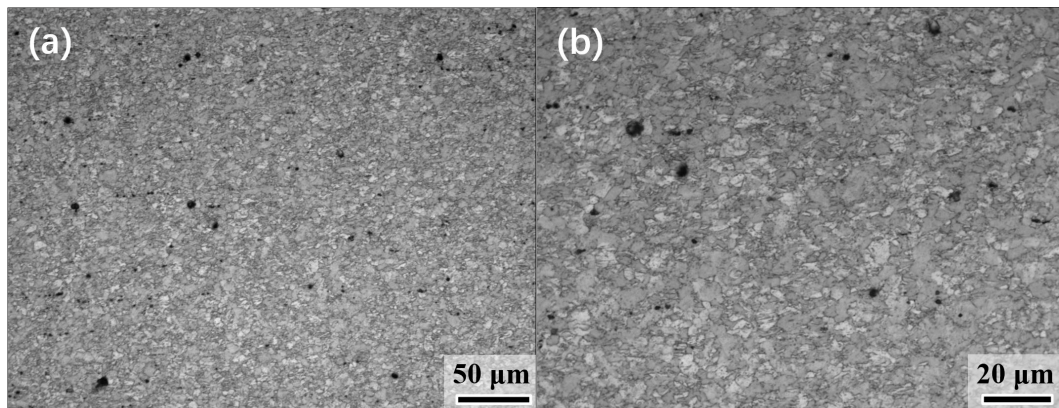


Figure 5. (a) Low power and (b) high power LM micrographs of the E-Cred BX11 alloy.

In order to further investigate the microstructure of the E-Cred BX11 alloy, TEM experiments were carried out. TEM images and corresponding selected area electron diffraction (SAED) patterns of caliber rolling-processed samples with different resolutions are shown in Figure 6. Figure 6a presents the dark field TEM image of the E-Cred BX11 alloy together with the corresponding SAED patterns exhibiting diffraction rings (inserted in Figure 6a), which indicates that the sample contains nano-scaled grains with high-angle grain boundaries. In Figure 6b and c, the bright field TEM image clearly demonstrates that three-pass caliber rolling produces ultra-fine grains with sizes of ~200 nm. Besides, as indicated by green arrows in Figure 6b and c, many sub-grains can be detected near the ultra-fine grain area, and some nano precipitates are found to stay along or nearby the residual dislocation lines. Based on the represented EDX result in Figure 6d, the precipitate is rich of Mg and Ca, similar with those in the as-extruded BX11 sample, which is conformed as the Mg_2Ca phase in our former research [17]. Moreover, as observed in Figure 6d, residual dislocation lines are readily detected, and these robustly generated dislocations during caliber rolling have partially transformed into sub-grains, as indicated by the yellow arrows in Figure 6d. It is thus hypothetical that the sub-grain boundaries and the residual dislocations induced by caliber-rolling processing play the critical role in generating the potential nuclei of the recrystallization [9,36]. In addition, these nano-precipitated particles are found to be distributed at the DRXed sub-grain boundaries (Figure 6d), which can contribute to the formation of the ultra-fine grains to some extent through the pinning effect on grain boundary movement in the present caliber-rolling conditions. Surprisingly, the ultra-fine grain size of the E-Cred BX11 alloy is comparable with that obtained by SPD-processed Mg alloys, such as the 18-pass ECAPed AZ31 [21], ARBed AZ91 [23], 12-pass ECAPed Mg-3.7Al-1.8Ca-0.4Mn [24], Deed Mg-0.5Ca [10], and even the RE-containing Mg-10Gd-5.7Y-0.5Zr [28] alloys. Accordingly, the bimodal microstructure containing submicron grains and sub-grains and residual dislocations, as well as microscale and nanoscale second phase particles, will inevitably contribute to the high strength of the present E-Cred BX11 alloy.

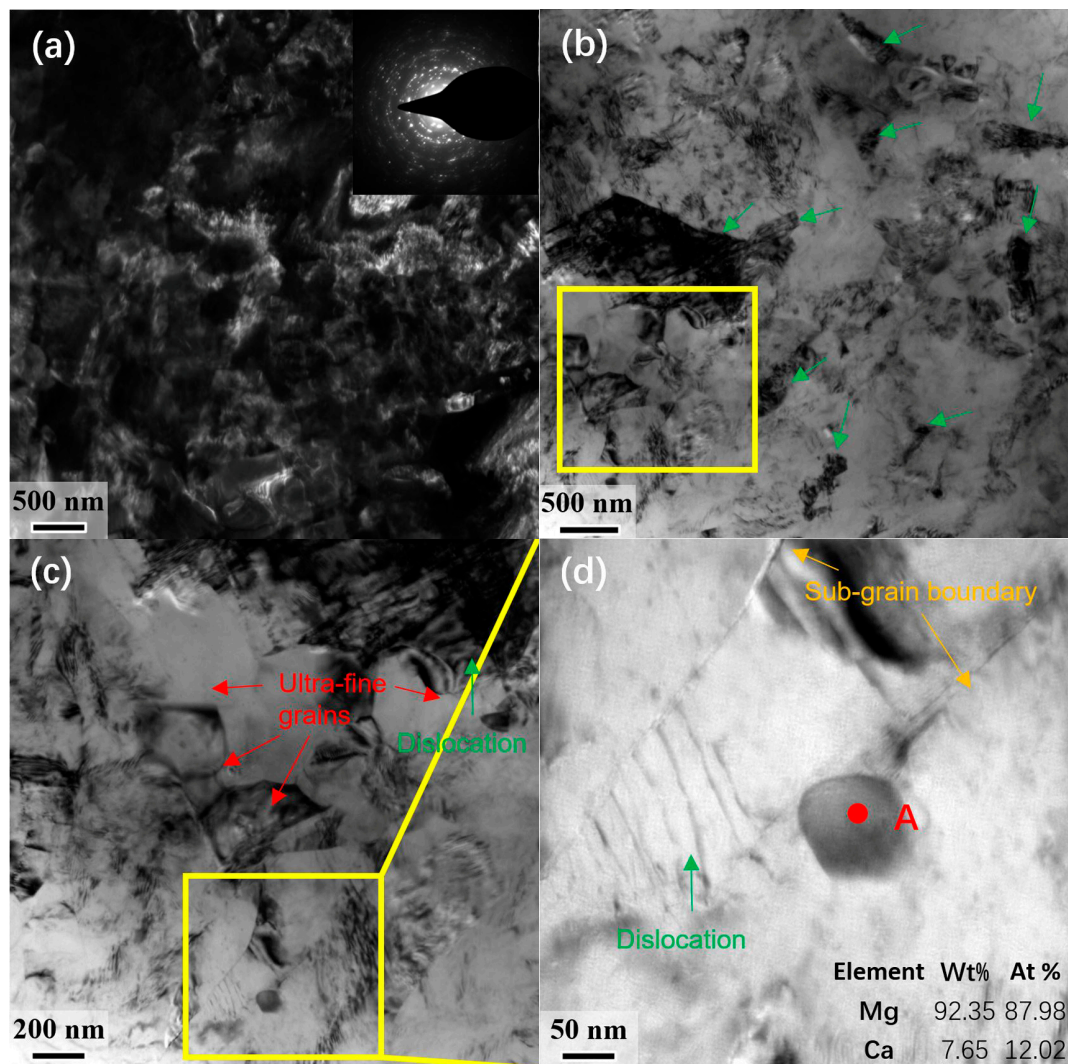


Figure 6. (a) Dark field TEM image and corresponding selected area electron diffraction (SAED) pattern of the E-CRed sample, and (b–d) bright field images and energy-dispersive X-ray spectroscopy (EDX) results of the precipitate.

Figure 7 shows the EBSD analysis results of the E-CRed BX11 alloy. After three-pass caliber rolling, both the deformed coarse grains with the volume fractions of ~55% and ultra-fine grains with diameters less than 1 μm can be seen clearly in the inverse pole figure (IPF) maps (Figure 7a–c). This bimodal microstructure is well agreed with the LM observation. In addition, the E-CRed BX11 alloy exhibits basal texture (Figure 7d–f), which means that the $\{0001\}$ plane are mainly oriented parallel to the RD. The texture type is significantly different from the “RE” texture of the as-extruded sample [17]. In addition, the maximum texture intensity (I_{max}) of the E-CRed sample is 8.64 multiples the uniform density (mud.), which is much stronger than that of the sample free of rolling. It should be noted that the deformed grains in the E-CRed sample demonstrate strong textures, with the $\{0001\}$ plane direction mainly oriented parallel to the RD, while a different texture type is generated with the ultra-fine DRXed grains, the intensity of which is only half of that of the deformed grains, as indicated in Figure 7e,f. The result is consistent with previous research results of the texture components transition during DRX [15]. The basal texture intensity of E-CRed BX11 alloy is much higher than that of the as-extruded BAZ811 ($I_{\text{max}} = 3.7$) [15], Mg-6Bi ($I_{\text{max}} = 4.5$) [16], and as-extruded BX11 [17] alloys, and even stronger than the LTSS-Eed bimodal AZ80 alloy ($I_{\text{max}} = 5.1$) [30], indicating that the texture of the extruded alloy greatly depends on not only the alloy composition but also the processing route. It can be expected

that the strong basal texture can inevitably strengthen the alloy by suppressing the basal slip during the tensile test along the RD [5,29]. Interestingly, the necklace-like structure with fine DRXed grains formed around the deformed grains can be readily observed in the microstructure, indicating the discontinuous DRX during caliber rolling. As a result, a bulk Mg alloy having necklace-like structure with strong basal texture was successfully fabricated by combining two simple thermomechanical processes in the present study.

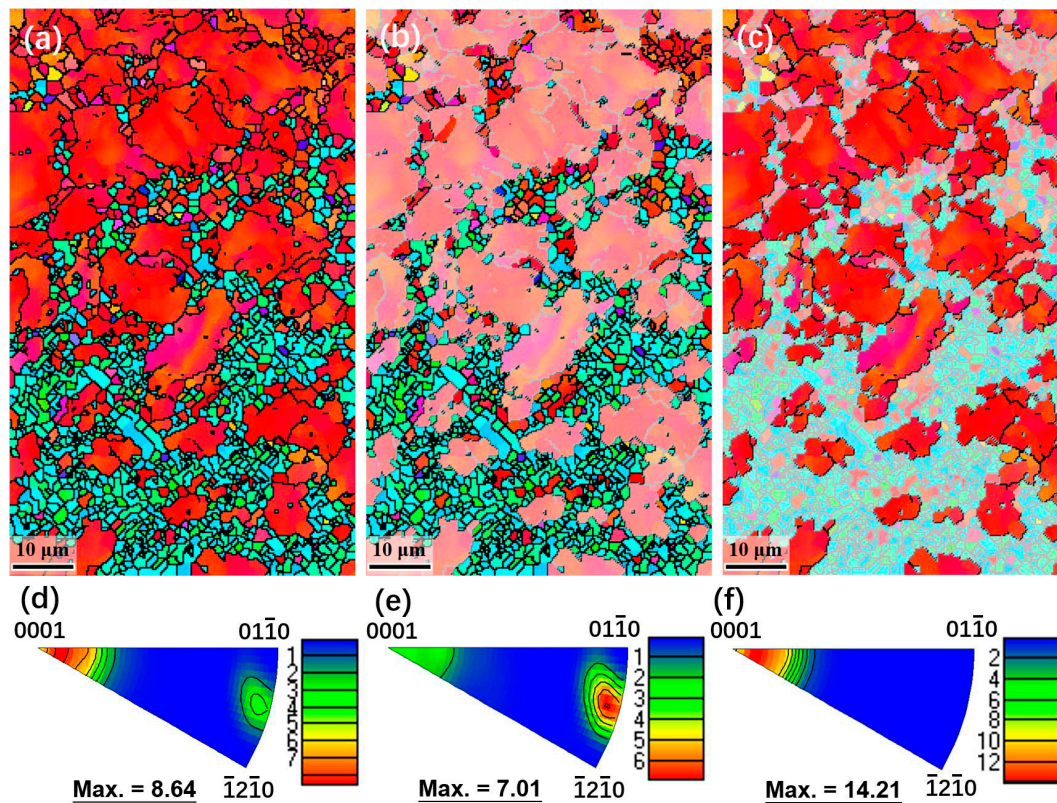


Figure 7. (a,b,c) Inverse pole figure maps and (d,e,f) inverse pole figures of the E-CRed BX11 alloy; (a,d) overall, (b,e) un-DRXed, and (e,f) DRXed regions.

Furthermore, as shown in Figure 8 [4,5,10,11,15,16,19,21–34], the E-CRed BX11 alloy with dilute cheap alloying elements demonstrates excellent tensile properties compared with the other high-strength Mg alloys. Based on the above microstructure characterization of the E-CRed BX11, its high strength and good ductility are mainly attribute to the necklace-like bimodal structure, which is reported to be beneficial to both the strength and ductility. The good combination of both high strength and high ductility was also observed in a necklace-like bimodal-structured Mg-9Al-1Zn processed by hard plate rolling (HPR) [29]. It has been proposed as one strategy to achieve high-strength ductile materials by developing a bimodal microstructure, where the ultra-fine grains provide high strength while the coarser grains enable strain-hardening by providing more space to accommodate dislocations [37–39]. As to the texture strengthening, the much stronger basal texture of the E-CRed BX11 alloy will inevitably contribute to the high strength by restricting the activation of the dislocation slip and, at the same time, decrease its ductility [40,41]. Besides, the ultra-high strength of the E-CRed BX11 will be slightly further enhanced by precipitation-strengthening from fine Mg_2Ca precipitates and the dispersion-strengthening from relatively large Mg_3Bi_2 and $\text{Mg}_2\text{Bi}_2\text{Ca}$ phases, as well as solid-solution-strengthening from dissolved Ca and Bi.

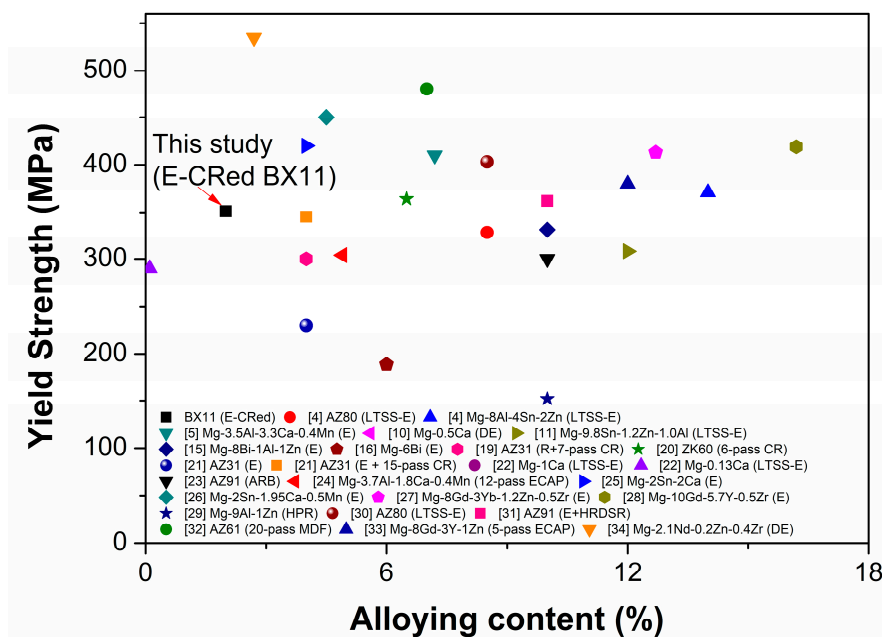


Figure 8. Comparison of YS vs. alloying content of E-CRed BX11 alloy with reported various wrought Mg alloys [4,5,10,11,15,16,19,21–34].

4. Conclusions

In summary, we successfully enhanced the strength of a dilute BX11 alloy by three-pass caliber rolling. The RE-free E-CRed BX11 alloy exhibits a high YS of ~351 MPa and, at same time, a good ductility of ~13.2%. The excellent mechanical properties are mainly attributed to the combined results of grain refinement and texture-strengthening from the bimodal structure. Overall, the dilute alloying elements and the simple-processing technology of the combination of the commercially accepted, both, conventional extrusion and caliber rolling are expected to inspire the new alloy design strategy and processing method for fabricating high-performance Mg products for larger-scale industrial applications.

Author Contributions: Methodology, S.M., H.Y., and H.H.; data curation, S.M., J.F., L.H., and L.D.; formal analysis, Z.L.; investigation, S.M., H.Y., H.H., L.D., X.N., and Z.L.; resources, H.H., X.N., Z.L., S.H.P., and W.Z.; writing—original draft preparation, S.M. and H.Y.; writing—review and editing, S.M., H.Y., H.H., J.F., L.H., L.D., X.N., Z.L., S.H.P., and W.Z.; supervision, H.Y., H.H., L.D., and W.Z.; and project administration, W.Z. and H.Y. All authors have read and agreed to the published version of the manuscript.

Funding: The authors acknowledge financial support from the National Natural Science Foundation of China (51701060 and 51601181), the Natural Science Foundation of Tianjin city (18JCQNJC03900), the Scientific Research Foundation for the Returned Overseas Chinese Scholars of Hebei Province (C20190505), the 100 Foreign Experts Plan of Hebei Province (141100), the Foundation Strengthening Program (2019-JCJQ-142), the National Research Council of Science & Technology (NST) grant by the Korean government (MSIP) (CRC-15-06-KIGAM), and the Joint Doctoral Training Foundation of HEBUT (2018HW0008).

Conflicts of Interest: The authors declare no conflicts of interest.

References

1. Suh, B.C.; Shim, M.S.; Shin, K.S.; Kim, N.J. Current issues in magnesium sheet alloys: Where do we go from here? *Scr. Mater.* **2014**, *84–85*, 1–6. [CrossRef]
2. Meng, S.J.; Yu, H.; Fan, S.D.; Li, Q.Z.; Park, S.H.; Suh, J.S.; Kim, Y.M.; Nan, X.L.; Bian, M.Z.; Yin, F.X.; et al. Recent Progress and Development in Extrusion of Rare Earth Free Mg Alloys. *Acta Metall. Sin. (Engl. Lett.)* **2019**, *32*, 145–168. [CrossRef]
3. Lee, T.; Shih, D.S.; Lee, Y.; Lee, C.S. Manufacturing Ultrafine-Grained Ti-6Al-4V Bulk Rod Using Multi-Pass Caliber-Rolling. *Metals* **2015**, *5*, 777–789. [CrossRef]

4. Park, S.H.; Jung, J.G.; Kim, Y.M.; You, B.S. A new high-strength extruded Mg-8Al-4Sn-2Zn alloy. *Mater. Lett.* **2015**, *139*, 35–38. [[CrossRef](#)]
5. Xu, S.W.; Oh-ishi, K.; Kamado, S.; Uchida, F.; Homma, T.; Hono, K. High-strength extruded Mg-Al-Ca-Mn alloy. *Scr. Mater.* **2011**, *65*, 269–272. [[CrossRef](#)]
6. Homma, T.; Mendis, C.L.; Hono, K.; Kamado, S. Effect of Zr addition on the mechanical properties of as-extruded Mg-Zn-Ca-Zr alloys. *Mater. Sci. Eng. A* **2010**, *527*, 2356–2362. [[CrossRef](#)]
7. Qi, F.; Zhang, D.; Zhang, X.; Xu, X. Effect of Sn addition on the microstructure and mechanical properties of Mg-6Zn-1Mn (wt %) alloy. *J. Alloys Compd.* **2014**, *585*, 656–666. [[CrossRef](#)]
8. Zhang, D.-F.; Shi, G.-L.; Dai, Q.-W.; Yuan, W.; Duan, H.-L. Microstructures and mechanical properties of high strength Mg-Zn-Mn alloy. *Trans. Nonferrous Met. Soc. China* **2008**, *18*, S59–S63. [[CrossRef](#)]
9. Pan, H.; Qin, G.; Ren, Y.; Wang, L.; Sun, S.; Meng, X. Achieving high strength in indirectly-extruded binary Mg-Ca alloy containing Guinier-Preston zones. *J. Alloys Compd.* **2015**, *630*, 272–276. [[CrossRef](#)]
10. Ikeo, N.; Nishioka, M.; Mukai, T. Fabrication of biodegradable materials with high strength by grain refinement of Mg-0.3 at % Ca alloys. *Mater. Lett.* **2018**, *223*, 65–68. [[CrossRef](#)]
11. Sasaki, T.T.; Yamamoto, K.; Honma, T.; Kamado, S.; Hono, K. A high-strength Mg-Sn-Zn-Al alloy extruded at low temperature. *Scr. Mater.* **2008**, *59*, 1111–1114. [[CrossRef](#)]
12. Sasaki, T.T.; Elsayed, F.R.; Nakata, T.; Ohkubo, T.; Kamado, S.; Hono, K. Strong and ductile heat-treatable Mg-Sn-Zn-Al wrought alloys. *Acta Mater.* **2015**, *99*, 176–186. [[CrossRef](#)]
13. Remennik, S.; Bartsch, I.; Willbold, E.; Witte, F.; Shechtman, D. New, fast corroding high ductility Mg-Bi-Ca and Mg-Bi-Si alloys, with no clinically observable gas formation in bone implants. *Mater. Sci. Eng. B* **2011**, *176*, 1653–1659. [[CrossRef](#)]
14. Somekawa, H.; Singh, A. Superior room temperature ductility of magnesium dilute binary alloy via grain boundary sliding. *Scr. Mater.* **2018**, *150*, 26–30. [[CrossRef](#)]
15. Meng, S.; Yu, H.; Zhang, H.; Cui, H.; Park, S.H.; Zhao, W.; You, B.S. Microstructure and mechanical properties of an extruded Mg-8Bi-1Al-1Zn (wt %) alloy. *Mater. Sci. Eng. A* **2017**, *690*, 80–87. [[CrossRef](#)]
16. Meng, S.; Yu, H.; Zhang, H.; Cui, H.; Wang, Z.; Zhao, W. Microstructure and mechanical properties of extruded pure Mg with Bi addition. *Acta Mater. Sin.* **2016**, *52*, 811–820.
17. Meng, S.J.; Yu, H.; Fan, S.D.; Kim, Y.M.; Park, S.H.; Zhao, W.M.; You, B.S.; Shin, K.S. A high-ductility extruded Mg-Bi-Ca alloy. *Mater. Lett.* **2020**, *261*, 127066. [[CrossRef](#)]
18. Somekawa, H.; Singh, A.; Inoue, T. Enhancement of toughness by grain boundary control in magnesium binary alloys. *Mater. Sci. Eng. A* **2014**, *612*, 172–178. [[CrossRef](#)]
19. Lee, J.H.; Kwak, B.J.; Kong, T.; Park, S.H.; Lee, T. Improved tensile properties of AZ31 Mg alloy subjected to various caliber-rolling strains. *J. Magnes. Alloy.* **2019**, *7*, 381–387. [[CrossRef](#)]
20. Lee, T.; Kwak, B.J.; Kong, T.; Lee, J.H.; Lee, S.W.; Park, S.H. Enhanced yield symmetry and strength-ductility balance of caliber-rolled Mg-6Zn-0.5Zr with ultrafine-grained structure and bulk dimension. *J. Alloys Compd.* **2019**, *803*, 434–441. [[CrossRef](#)]
21. Mukai, T.; Somekawa, H.; Inoue, T.; Singh, A. Strengthening Mg-Al-Zn alloy by repetitive oblique shear strain with caliber roll. *Scr. Mater.* **2010**, *62*, 113–116. [[CrossRef](#)]
22. Pan, H.; Yang, C.; Yang, Y.; Dai, Y.; Zhou, D.; Chai, L.; Huang, Q.; Yang, Q.; Liu, S.; Ren, Y.; et al. Ultra-fine grain size and exceptionally high strength in dilute Mg-Ca alloys achieved by conventional one-step extrusion. *Mater. Lett.* **2019**, *237*, 65–68. [[CrossRef](#)]
23. Miura, H.; Maruoka, T.; Yang, X.; Jonas, J.J. Microstructure and mechanical properties of multi-directionally forged Mg-Al-Zn alloy. *Scr. Mater.* **2012**, *66*, 49–51. [[CrossRef](#)]
24. Wang, C.; Ma, A.; Sun, J.; Zhuo, X.; Huang, H.; Liu, H.; Yang, Z.; Jiang, J. Improving Strength and Ductility of a Mg-3.7Al-1.8Ca-0.4Mn Alloy with Refined and Dispersed Al₂Ca Particles by Industrial-Scale ECAP Processing. *Metals* **2019**, *9*, 767. [[CrossRef](#)]
25. Pan, H.; Qin, G.; Huang, Y.; Ren, Y.; Sha, X.; Han, X.; Liu, Z.-Q.; Li, C.; Wu, X.; Chen, H.; et al. Development of low-alloyed and rare-earth-free magnesium alloys having ultra-high strength. *Acta Mater.* **2018**, *149*, 350–363. [[CrossRef](#)]
26. Zhang, A.; Kang, R.; Wu, L.; Pan, H.; Xie, H.; Huang, Q.; Liu, Y.; Ai, Z.; Ma, L.; Ren, Y.; et al. A new rare-earth-free Mg-Sn-Ca-Mn wrought alloy with ultra-high strength and good ductility. *Mater. Sci. Eng. A* **2019**, *754*, 269–274. [[CrossRef](#)]

27. Li, B.; Guan, K.; Yang, Q.; Niu, X.; Zhang, D.; Lv, S.; Meng, F.; Huang, Y.; Hort, N.; Meng, J. Microstructures and mechanical properties of a hot-extruded Mg-8Gd-3Yb-1.2Zn-0.5Zr (wt %) alloy. *J. Alloys Compd.* **2019**, *776*, 666–678. [[CrossRef](#)]
28. Homma, T.; Kunito, N.; Kamado, S. Fabrication of extraordinary high-strength magnesium alloy by hot extrusion. *Scr. Mater.* **2009**, *61*, 644–647. [[CrossRef](#)]
29. Zha, M.; Zhang, X.H.; Zhang, H.; Yao, J.; Wang, C.; Wang, H.Y.; Feng, T.T.; Jiang, Q.C. Achieving bimodal microstructure and enhanced tensile properties of Mg-9Al-1Zn alloy by tailoring deformation temperature during hard plate rolling (HPR). *J. Alloys Compd.* **2018**, *765*, 1228–1236. [[CrossRef](#)]
30. Yu, H.; Park, S.H.; You, B.S. Development of extraordinary high-strength Mg-8Al-0.5Zn alloy via a low temperature and slow speed extrusion. *Mater. Sci. Eng. A* **2014**, *610*, 445–449. [[CrossRef](#)]
31. Pérez-Prado, M.T.; del Valle, J.A.; Ruano, O.A. Achieving high strength in commercial Mg cast alloys through large strain rolling. *Mater. Lett.* **2005**, *59*, 3299–3303. [[CrossRef](#)]
32. Kim, W.J.; Jeong, H.G.; Jeong, H.T. Achieving high strength and high ductility in magnesium alloys using severe plastic deformation combined with low-temperature aging. *Scr. Mater.* **2009**, *61*, 1040–1043. [[CrossRef](#)]
33. Garces, G.; Pérez, P.; Barea, R.; Medina, J.; Stark, A.; Schell, N.; Adeva, P. Increase in the Mechanical Strength of Mg-8Gd-3Y-1Zn Alloy Containing Long-Period Stacking Ordered Phases Using Equal Channel Angular Pressing Processing. *Metals* **2019**, *9*, 221. [[CrossRef](#)]
34. Huang, H.; Miao, H.; Yuan, G.; Wang, Z.; Ding, W. Fabrication of ultra-high strength magnesium alloys over 540 MPa with low alloying concentration by double continuously extrusion. *J. Magnes. Alloy.* **2018**, *6*, 107–113. [[CrossRef](#)]
35. Tok, H.Y.; Hamzah, E.; Bakhsheshi-Rad, H.R. The role of bismuth on the microstructure and corrosion behavior of ternary Mg-1.2Ca-xBi alloys for biomedical applications. *J. Alloys Compd.* **2015**, *640*, 335–346. [[CrossRef](#)]
36. Oh-ishi, K.; Mendis, C.L.; Homma, T.; Kamado, S.; Ohkubo, T.; Hono, K. Bimodally grained microstructure development during hot extrusion of Mg-2.4 Zn-0.1 Ag-0.1 Ca-0.16 Zr (at %) alloys. *Acta Mater.* **2009**, *57*, 5593–5604. [[CrossRef](#)]
37. Wang, Y.; Chen, M.; Zhou, F.; Ma, E. High tensile ductility in a nanostructured metal. *Nature* **2002**, *419*, 912–915. [[CrossRef](#)]
38. Wang, Y.M.; Ma, E. Three strategies to achieve uniform tensile deformation in a nanostructured metal. *Acta Mater.* **2004**, *52*, 1699–1709. [[CrossRef](#)]
39. Witkin, D.; Lee, Z.; Rodriguez, R.; Nutt, S.; Lavernia, E. Al-Mg alloy engineered with bimodal grain size for high strength and increased ductility. *Scr. Mater.* **2003**, *49*, 297–302. [[CrossRef](#)]
40. Wang, H.Y.; Yu, Z.P.; Zhang, L.; Liu, C.G.; Zha, M.; Wang, C.; Jiang, Q.C. Achieving high strength and high ductility in magnesium alloy using hard-plate rolling (HPR) process. *Sci. Rep.* **2015**, *5*, 17100. [[CrossRef](#)]
41. Yamasaki, M.; Hashimoto, K.; Hagihara, K.; Kawamura, Y. Effect of multimodal microstructure evolution on mechanical properties of Mg-Zn-Y extruded alloy. *Acta Mater.* **2011**, *59*, 3646–3658. [[CrossRef](#)]

